2011

Cooperative effects in the oxidation of CO by palladium oxide cations

Arthur C. Reber
Virginia Commonwealth University, acreber@vcu.edu

Shiv N. Khanna
Virginia Commonwealth University, snkhanna@vcu.edu

Eric C. Tyo
Pennsylvania State University

Christopher L. Harmon
Pennsylvania State University

A. W. Castleman Jr
Pennsylvania State University

Reber, A. C., Khanna, S. N., & Tyo, E. C., et al. Cooperative effects in the oxidation of CO by palladium oxide cations. The Journal of Chemical Physics, 135, 234303 (2011). Copyright © 2011 American Institute of Physics.

Cooperative effects in the oxidation of CO by palladium oxide cations

Arthur C. Reber,[1] Shiv N. Khanna,[1,a)] Eric C. Tyo,[2] Christopher L. Harmon,[2] and A. W. Castleman, Jr.[2]
[1]*Department of Physics, Virginia Commonwealth University, 701 W. Grace St., Richmond, Virginia 23284-2000, USA*
[2]*Department of Chemistry and Physics, Pennsylvania State University, 104 Chemistry Research Building, University Park, Pennsylvania 16802, USA*

(Received 26 September 2011; accepted 16 November 2011; published online 19 December 2011)

Cooperative reactivity plays an important role in the oxidation of CO to CO_2 by palladium oxide cations and offers insight into factors which influence catalysis. Comprehensive studies including guided-ion-beam mass spectrometry and theoretical investigations reveal the reaction products and profiles of PdO_2^+ and PdO_3^+ with CO through oxygen radical centers and dioxygen complexes bound to the Pd atom. O radical centers are more reactive than the dioxygen complexes, and experimental evidence of both direct and cooperative CO oxidation with the adsorption of two CO molecules are observed. The binding of multiple electron withdrawing CO molecules is found to increase the barrier heights for reactivity due to decreased binding of the secondary CO molecule, however, reactivity is enhanced by the increase in kinetic energy available to hurdle the barrier. We examine the effect of oxygen sites, cooperative ligands, and spin including two-state reactivity.
 [doi:10.1063/1.3669428]

INTRODUCTION

Palladium is an important oxidation catalyst employed in a wide range of catalytic applications including CO oxidation, cracking of hydrocarbons, and other industrial processes.[1–10] Understanding the microscopic mechanisms that control its reactivity is therefore an important objective that could lead to the development of superior and alternate catalysts.[11–14] While most catalytic applications involve large free or supported nanoparticles, gas-phase studies on smaller clusters under controlled conditions are of great value because they enable the attainment of molecular level detail of reactions with atomic level precision.[15–20] Small cluster sizes are also amenable to *ab-initio* theoretical studies that can provide information on the atomic and electronic structure, nature of adsorption, reaction barriers, and the microscopic reaction mechanism. In combination with the experimental information, the synergistic effort can offer an atomistic understanding of the catalytic processes including the role of charge, size, stoichiometry, spin, and cooperative processes.

Recent experimental studies on Pd_n clusters supported on $TiO_2(110)$ have indicated that O_2 is dissociatively adsorbed on clusters containing 2 or more atoms, while the O_2 molecule is only activated on a single Pd atom.[21–23] Hence, oxidation studies on PdO_n^+ clusters containing 2 and 3 oxygen atoms may provide information on the behavior of activated oxygen, O radicals and other effects which have been studied extensively in transition metal oxides.[24–28] In this work, we present a synergistic study combining guided-ion-beam mass spectrometry experiments and theoretical investigations on the reactivity of palladium oxide cations with CO. Our focus on PdO_2^+ and PdO_3^+ is due to PdO_2^+ having a ground state with an undissociated and activated O_2 molecule, while the PdO_3^+ cluster has an activated O_2 molecule as well as a radical O center in its ground state. Hence, they offer the unique opportunity to delineate the role of activated oxygen and the O radical sites. We also investigate the effect of spin on the reactivity since two-state reactivity in which the optimal reaction profile involves a spin crossing has been found to be important in many transition metal oxide reactions.[29] While studies have been performed on numerous transition metal oxides, such studies on palladium oxide clusters are scarce.[30–32] Finally, we examine the cooperative oxidation processes[33] where the first CO is bound to the Pd site while a second CO undergoes the oxidation reaction. The adsorption of ligands such as CO can provide excess energy that can allow reactions to overcome barriers. What has not been emphasized previously is the effect of such additions on the reaction barriers.

In this paper, we combine guided-ion-beam mass spectrometry studies with theoretical investigations to study the reactivity of CO with PdO_2^+ and PdO_3^+. We first examine the structures and available active sites in the palladium oxide clusters. We then examine the reaction products of the experiment. We further examine the reaction profiles using first-principles theoretical methods. Finally, we examine the effect of spin on reactivity, and the effect of different CO and O groups to further understand the cooperative reactivity that is observed.

EXPERIMENTAL METHODS

The reactivity of PdO_2^+ and PdO_3^+ with CO was studied utilizing a guided-ion-beam mass spectrometer which has been thoroughly described in a previous publication.[34] In brief, palladium oxide clusters were produced in a laser vaporization (LaVa) source via pulsing of an expansion gas,

a)Authors to whom correspondence should be addressed. Electronic addresses: Snkhanna@vcu.edu and Awc@psu.edu.

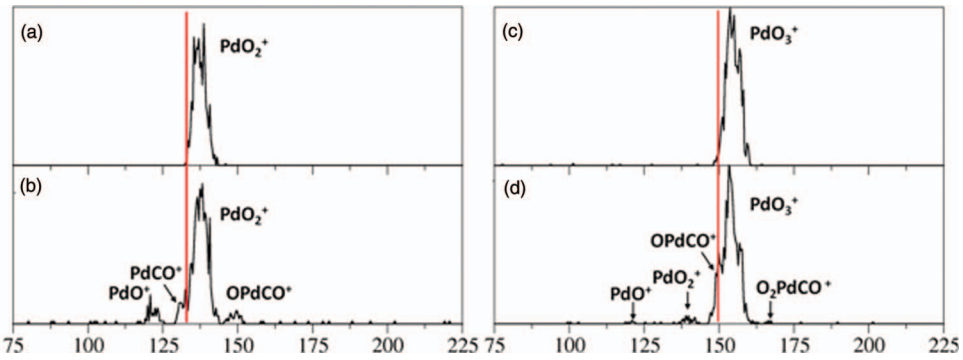

FIG. 1. (a) Mass spectra of PdO_2^+ and (b) the mass spectra of PdO_2^+ interacting with 5.97 mTorr CO. (c) Mass spectra of PdO_3^+ and (d) the mass spectra of PdO_3^+ interacting with 5.05 mTorr CO. The red lines mark the left edge of the PdO_2^+ and PdO_3^+ peaks, respectively.

composed of 5% oxygen seeded in helium, into the plasma created via ablation of a palladium rod by the second harmonic (532 nm) of a Nd:YAG laser. A conical expansion nozzle is attached to the exit of the LaVa source which aids in creation of larger and more oxygen rich clusters.[35] The clusters exit the LaVa source and are cooled by supersonic expansion into vacuum. The high pressure of the expansion gas (13.2 atm) passing into a low pressure field free region decreases the internal vibrational and rotational energy of the clusters through three-body collisions. A retarding potential analysis previously performed in our laboratory has determined that the energy imparted upon the clusters exiting the LaVa source is around 1 eV in the laboratory frame.[25] The clusters progress through a 3 mm skimmer creating a collimated molecular beam and are directed by a set of electrostatic lenses into a quadrupole mass filter. The quadrupole mass filter permits clusters of a desired mass to charge (m/z) ratio to pass into an octopole collision cell. Varying pressures of CO are admitted to the collision cell utilizing a low flow leak valve to probe the reactivity and structural characteristics of the clusters. An mks Baratron capacitance manometer is used to monitor the pressure of reactant introduced. The injection lens before the collision cell and the dc float voltage applied to the octopole ion guide are grounded so the clusters react at thermal energies. The product ions are extracted from the octopole and flow into a second quadrupole mass filter, which scans a (m/z) range of 40–740 amu to perform product mass determination. Lastly, resultant ions are detected by a channel electron multiplier connected to a multichannel scalar card. The mass spectra presented in Figure 1 display the reaction products for the interaction of PdO_2^+ and PdO_3^+ with CO. To aid in the observation of shoulder-peaks the spectra of mass selected parent ions is presented above the spectrum recorded during interaction between ion and reactant molecule. A red line indicates the separation between a peak and shoulder-peak.

THEORETICAL METHODS

Theoretical investigations on the structural properties of PdO_n^+ where n = 2, 3 and their reactivity with CO were performed within a gradient corrected density functional formalism. The calculations were carried out using the deMon2k (Ref. 36) set of codes while using the PBE generalized gradient approximation[37] for exchange and correlation. The palladium atom is described using a 18 electron quasi-relativistic effective core potential[38] and the corresponding valence basis set as proposed by Andrae *et al.*[39] In a recent paper,[40] Köster *et al.* have shown that such a quasi-relativistic potential can lead to an accurate description of the binding and electronic states in Pd_n clusters. For O and C, the calculations were carried out at an all electron level and a TZVP basis[41] was used. Transition states were determined using the hierarchical transition state search algorithm.[42] The reaction profiles were calculated using density functional theory. All reasonable spin multiplicities were considered for the reactions and we examined both single-state and two-state reaction profiles.

RESULTS

Palladium oxide cation clusters, PdO_2^+ and PdO_3^+ have been experimentally and theoretically investigated to understand the reactivity of different oxygen centers bound to the Pd atom as well as the effect of different constituents bound to the Pd atom. Theoretical investigations identified the type of oxygen centers found on the PdO_n^+ clusters. Figures 2(a)–2(d) shows that PdO_2^+ prefers a structure with an O_2 molecule bound to the Pd atom. The O–O bond has stretched from 1.23 Å in isolation to 1.26 Å, and the spin density on the O atoms shift from 1.0 μ_b to 0.5 μ_b per atom from the molecule to the complex, indicating that the oxygen molecule is slightly activated by the Pd atom. The occupation of π^* orbitals in the complex is similar to that in a free O_2 molecule, and the charge on the O atoms are slightly positive by both a Mulliken and Hirshfeld charge analysis, as we are dealing with a cation. The hybridization with Pd does reduce the net spin and slightly stretches the O_2 bond. Because of this we will consider the O_2 group to be composed of a dioxygen complex, and not the more reactive O_2^- superoxide complex. The binding energy of the $^3O_2$ to the Pd^+ atom is 1.32 eV. The complex with a spin of 3 μ_b is 0.73 eV higher in energy as shown in Fig. 2(b). The isomer with the O–O bond broken is 2.16 eV higher in energy than with the O–O bond intact, and the energy of the 1 μ_b and 3 μ_b isomers are essentially identical. In the isomers with a broken O–O bond, the spin density on the O atoms are greater than 1 μ_b indicating that the O

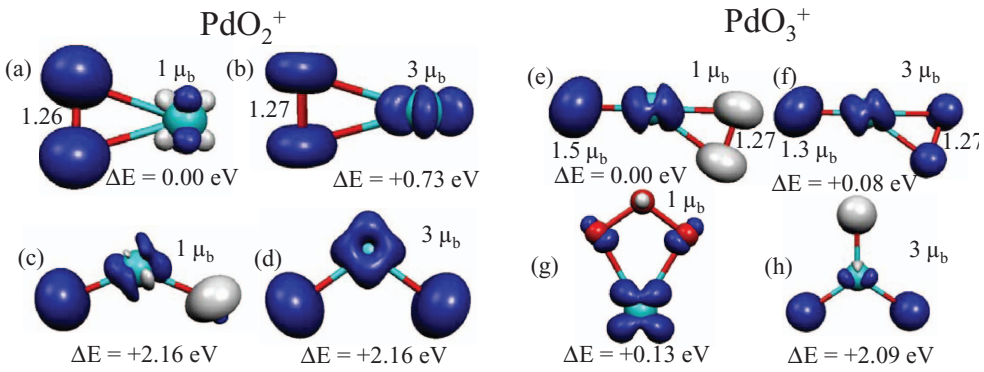

FIG. 2. Calculated structures for (a)-(d) PdO_2^+ and (e)-(h) PdO_3^+. The isosurfaces indicate spin density, with blue being spin up and gray spin down. Mulliken spin densities of the radical sites are listed in μ_b, and the O–O bond distances are marked in angstroms.

serves as a radical center. In PdO_3^+, the ground state structure has an activated O_2 molecule bound to the cluster, along with a radical oxygen center with a 1.5 μ_b spin charge, as shown in Fig. 2(e). The isomer, Fig. 2(f), with a 3 μ_b spin is only 0.08 eV higher in energy making it likely to be observed in experiments. A second isomer with an ozone molecule bound to the Pd atom is also close in energy at 0.13 eV higher than the ground state, and the structure with three separated oxygen atoms is 2.09 eV higher in energy, as shown in Figs. 2(g) and 2(h). The calculations reveal that PdO_2^+ serves as a model species with a bound O_2 molecule, while the PdO_3^+ serves as a model for species with a radical site.

Experimental data is presented as mass spectra in Figs. 1(a)–1(d). The spectra for the mass selected species PdO_2^+ without introduction of reactant is shown in Fig. 1(a). The width of the peak is due to the 6 palladium isotopes spanning a 9 amu range. To observe products of low intensity, the resolution of the mass spectrometer was lowered to a point at which isolation of isotopes was unfeasible. Figure 1(b) presents the mass spectra obtained upon interaction of 5.97 mTorr CO with PdO_2^+; the major products observed are $OPdCO^+$, $PdCO^+$, and PdO^+. Baseline resolution is not obtained between the parent PdO_2^+ and the $PdCO^+$ product due to the isotopic distribution of palladium yet the shoulder peak is observed and indicated by the red line. Single collision conditions are obtained below 0.8 mTorr. The experiment was conducted at higher pressures to investigate cooperative effects which occur when multiple reactants impinge upon the parent ion. The reaction mechanisms which lead to the observed products for PdO_2^+ are shown in Eqs. (1)–(3):

$$PdO_2^+ + CO \rightarrow PdCO^+ + O_2, \quad (1)$$

$$PdO_2^+ + CO \rightarrow PdO^+ + CO_2, \quad (2)$$

$$PdO_2^+ + 2CO \rightarrow OPdCO^+ + CO_2. \quad (3)$$

The $OCPdO_2^+$ peak is conspicuously absent indicating that simple binding of CO is not observed; if no reaction occurs, the complex breaks back into CO and PdO_2^+ before reaching the detector. Experiments were performed reacting PdO^+ with CO and the only product observed was $PdCO^+$, with loss of an O atom. This rules out the hypothesis that the $OPdCO^+$ peak is caused by reaction 2, followed by binding of a second CO molecule, as simple binding of CO is not observed in PdO^+. We also note that the binding of CO followed by loss of O is endothermic by 2.78 eV, which excludes associative detachment of CO with the loss of an O atom as the mechanism for formation of $OPdCO^+$.

In a similar fashion, the mass spectra for PdO_3^+ is presented in Fig. 1(c), while the result of interaction between 5.05 mTorr CO and PdO_3^+ is shown in the mass spectra Fig. 1(d). The products of discernable intensity are O_2PdCO^+, $OPdCO^+$, PdO_2^+, and PdO^+. The PdO^+ product is of negligible intensity and being such will not be considered further. The products are described by the following reactions (Eqs. (4)–(6)):

$$PdO_3^+ + CO \rightarrow OPdCO^+ + O_2, \quad (4)$$

$$PdO_3^+ + CO \rightarrow PdO_2^+ + CO_2, \quad (5)$$

$$PdO_3^+ + 2CO \rightarrow O_2PdCO^+ + CO_2. \quad (6)$$

As in PdO_2^+ peaks for the associative detachment of O_2 are observed and described by Eq. (4), as are direct oxidation of CO to CO_2 in Eq. (5), and cooperative oxidation of CO as shown in Eq. (6). The formation of O_2PdCO^+ is unlikely to be caused by consecutive reactions, as the binding of CO to PdO_2^+ will most likely result in the formation of $PdCO^+$, as seen in Fig. 1(b). The associative detachment of CO to PdO_3^+ with the loss of an O atom is endothermic by 0.45 eV while O_2 loss is exothermic by 0.61 eV, so this process for formation of O_2PdCO^+ is unlikely.

To examine the role of differing oxygen centers on the reactivity barriers and kinetics, we examine the reaction pathways for PdO_2^+ reaction with CO. A peak corresponding to replacement of O_2 by CO is observed in the mass spectra. Figure 3(a) shows this reaction, Eq. (1), which is barrierless and exothermic. The direct oxidation of CO to CO_2 (Eq. (2)) is shown in Fig. 3(b). The barrier for inserting the CO into the dioxygen group is 1.91 eV above the complex.

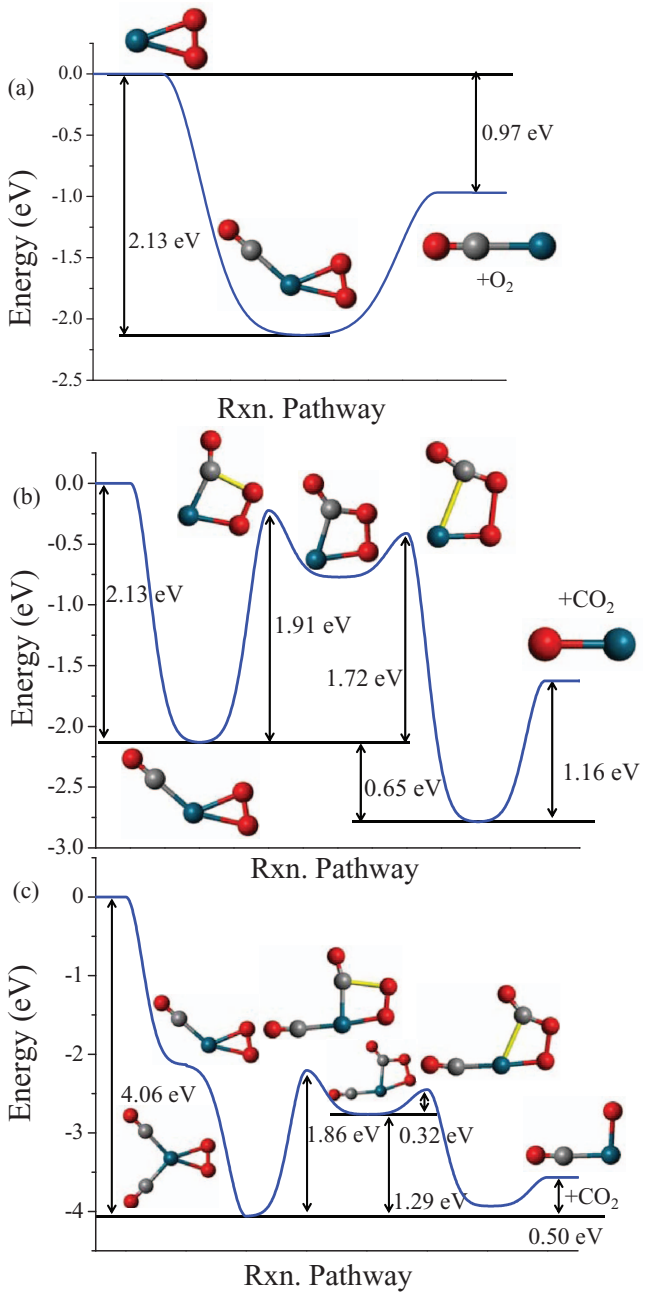

FIG. 3. Reaction pathways for the reaction of $^2PdO_2^+$ with CO. (a) O_2 loss, (b) CO oxidation to CO_2, and (c) CO oxidation through the binding of two CO molecules.

The binding energy of CO is 2.13 eV, so the barrier is 0.22 eV below the initial energy of the reactants indicating an energetically favorable process. Figure 3(c) shows the reaction pathway for CO oxidation in which two successive CO molecules are bound to the Pd atom as in Eq. (3). The binding energy of the first CO is 2.13 eV, and the second binds at 1.93 eV. The multiple adsorptions put significantly more energy into the complex, so the 1.86 eV barrier for CO insertion into the O_2 molecule is easily overcome.

For the interaction of CO with PdO_3^+, which contains both a radical oxygen center and an adsorbed oxygen molecule, we examine the two probable reaction pathways for the oxidation of CO. Figure 4(a) shows the reaction pathway in which the O_2 molecule is released after the adsorption of the CO molecule in accordance with Eq. (4). Figure 4(b) shows the reaction pathway for the oxidation of CO to CO_2 through the oxygen radical site as presented by Eq. (5). The barrier for reaction is 0.70 eV above the adsorption energy, and the loss of CO_2 is highly exothermic. The reaction pathway through the adsorbed oxygen molecule is shown in Fig. 4(c) and has a much higher barrier of 1.51 eV above the adsorption complex, 0.81 eV higher than through the radical center. There are two barriers to be overcome in this mechanism, first the insertion of CO into the O_2 complex, and then the cleaving of the Pd-C bond; we find the initial insertion to be the higher barrier. Figure 4(d) shows the reaction mechanism for the adsorption of two CO molecules leading to the oxidation of CO (Eq. (6)) at the O radical center. The binding of the first CO to PdO_3^+ is 1.78 eV, but the second binds at only 0.92 eV.

Next, we consider the effect of spin on the reaction profiles in PdO_3^+. The reaction pathways for $^2PdO_3^+$ and $^4PdO_3^+$ where CO attacks the radical site are shown in Fig. 5(a). The total energy of the barrier for CO insertion into the O radical center is 0.12 eV lower for $^4PdO_3^+$ than for $^2PdO_3^+$; however, the products attributed to the $^2PdO_3^+$ pathway are more stable. This suggests that two-state reactivity may play a role. Figure 5(b) shows the reaction profiles through the radical site with the adsorption of two CO molecules, and the profiles are again quite similar. Figure 5(c) shows the reaction profiles for insertion of CO into the dioxygen site of PdO_3^+, the barrier for $^4PdO_3^+$ is 0.08 eV higher than that for $^2PdO_3^+$. The barrier is even larger for the case with the adsorption of two CO molecules to PdO_3^+ (Fig. 5(d)) in which the $^2PdO_3^+$ channel is 0.45 eV lower in energy. We note that in the case of a single CO, the secondary barrier in which the O–O bond is broken is lower in the $^4PdO_3^+$ channel so again two-state reactivity may contribute. In general, changing the spin multiplicity of the reactants has a modest effect on the reaction barriers, so two-state reactivity[37] is likely to have some effect on the reaction rate, but it is generally small enough that we do not expect a major shift in the reactivity due to spin effects.

CO oxidation enhanced by the adsorption of multiple CO may result from the electronic effects which activate the oxygen molecule bound to the Pd atom, or they may be a result of the kinetic energy which binding CO puts into the system. To understand this effect, we plotted the energy of PdO_2^+ and $OCPdO_2^+$ as a function of the bond angle between the O atoms, as shown in Fig. S1.[43] We find that the adsorption of CO increases the barrier to O–O cleavage from 3.01 eV to 3.31 eV. This is due to the CO withdrawing charge from the PdO_2^+ complex resulting in a stronger O–O bond. We note that the barrier for the second pathway is 0.05 eV lower than in the first pathway, but in either case the effect on the position of the transition state is not significant. This implies that the increase in CO oxidation of Pd clusters with O_2 bound after the adsorption of two CO molecules is caused by an increase in energy rather than an electronic effect which changes the barrier heights. We note that in the cluster, the cooperative effects are enhancing the oxidation of CO in the gas phase, however, this behavior will be markedly different once the

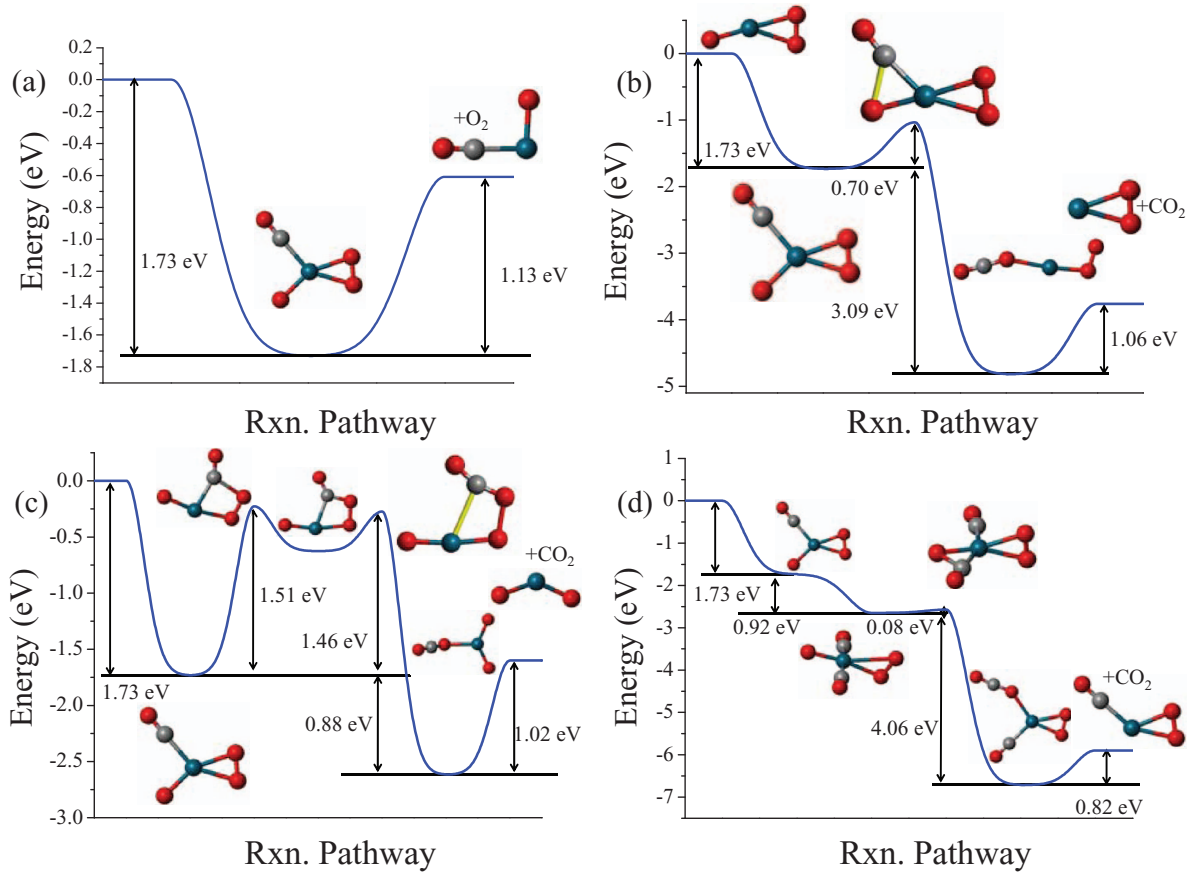

FIG. 4. Reaction pathways for the reaction of $^2PdO_3^+$ with CO. (a) O_2 loss, (b) CO oxidation to CO_2 through the O radical center, (c) CO oxidation through the O_2 site, and (d) CO oxidation with two CO bound to cluster.

cluster is deposited on a surface. In this case, the kinetic energy provided by binding the CO molecule to the cluster will dissipate rapidly while the increase in barrier height will remain. The result is the poisioning of the catalyst, and this multiple binding energies of CO to Pd clusters on surfaces has been observed.[44]

To further examine the effect of constituents on the barrier for insertion of CO into the dioxygen and O radical centers, we have tabulated all of the studied combinations and spin multiplicities in Table I. The first column shows the reaction barriers for the insertion into the dioxygen site. The calculated barrier has been compared to the free reactants and assumes spin conservation which is shown in Eq. (7) for the pure PdO_n complexes and Eq. (8) for the complexes with associated CO.

$$E(\text{barrier}) = E_{TS}(^mOCPdO_n^+) - E(^mPdO_n^+) - E(CO), \tag{7}$$

$$E(\text{barrier}) = E_{TS}(^m(OC)_2PdO_n^+) - E(^mOCPdO_n^+) - E(CO). \tag{8}$$

TABLE I. Reaction barrier heights as described by Eqs. (7) and (8) for the insertion of CO into dioxygen and O radical sites.

Species	Dioxygen site	Dioxygen+ associated CO	Radical	Radical+ associated CO
$^2PdO_2^+$	−0.22 eV	−0.07 eV	−1.60 eV	−0.89 eV
$^4PdO_2^+$	−0.11 eV	0.80 eV	−1.27 eV	−1.26 eV
$^2PdO_3^+$	−0.23 eV	−0.14 eV	−1.03 eV	−0.84 eV
$^4PdO_3^+$	−0.22 eV	0.24 eV	−1.23 eV	−0.85 eV

The clearest trend is that the dioxygen complexes with higher spin multiplicities have consistently higher barriers for insertion into the dioxygen unit than those with low spin multiplicities. The α-LUMO of $^2PdO_2^+$ and α-HOMO of $^4PdO_2^+$ have significant π^* character localized on the oxygen molecule which form antibonding orbitals with a 4*d* orbital of Pd, so the spin excitation results in the filling of this orbital with a weaker O_2-Pd interaction for $^4PdO_2^+$ and an increase in the barrier height. The one exception is in $^2PdO_3^+$ and $^4PdO_3^+$ which are found to have nearly identical barriers. $^2PdO_3^+$ has an antiferromagnetic ordering between the O radical and dioxygen complex, which results in the two multiplicities having a similar local spin moment, so changing the multiplicity has a minimal effect on the reactivity.

The addition of CO increases the barrier height for the reaction by 0.15 eV and 0.91 eV for the doublet and quartet multiplicities of PdO_2^+, and by 0.09 eV and 0.46 eV for the doublet and quartet multiplicities of PdO_3^+. The most active

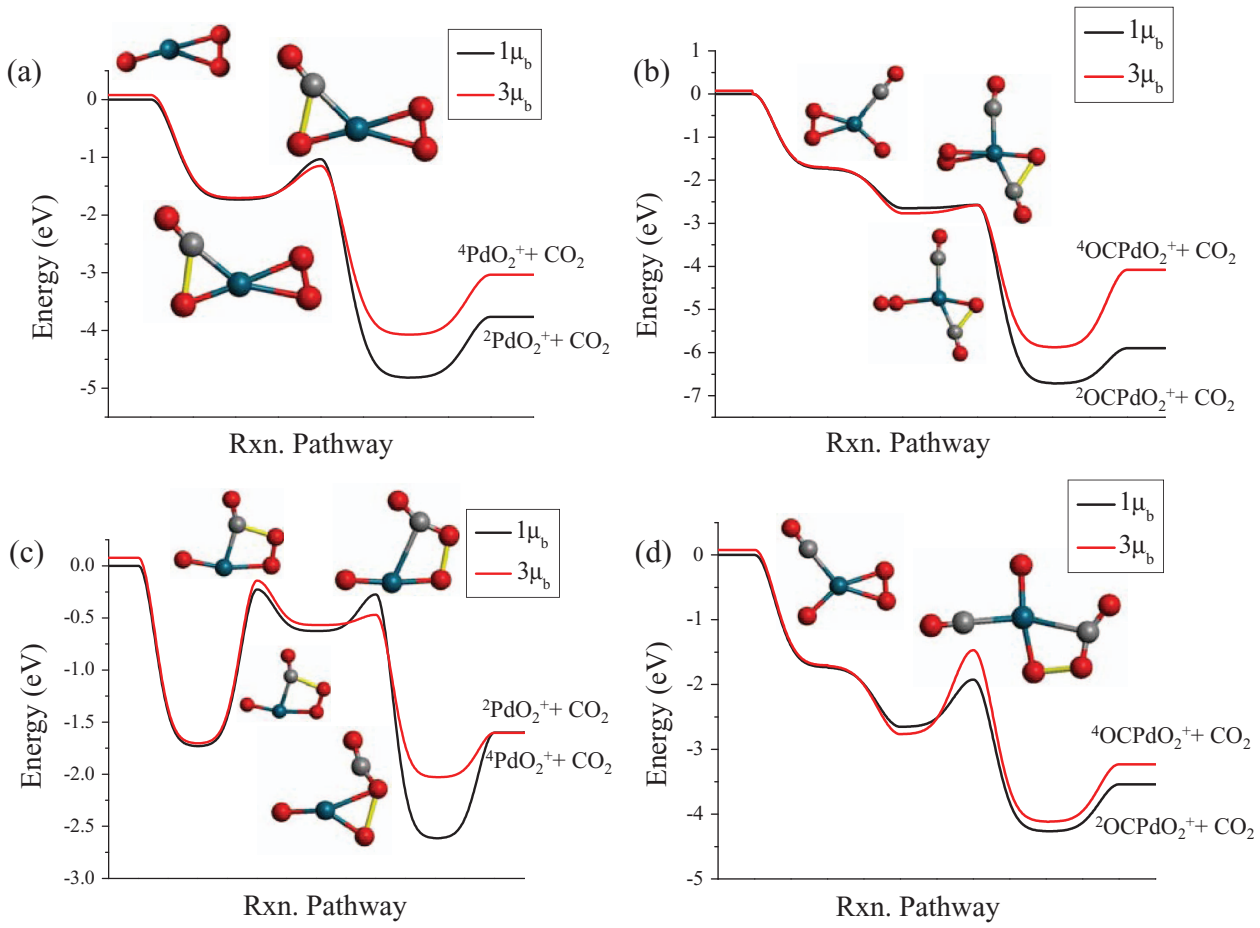

FIG. 5. Two-state reaction profiles for different spin multiplicities for (a) PdO_3^+ attacking the radical site, (b) PdO_3^+ binding two CO molecules and attacking the radical site, (c) PdO_3^+ with CO attacking the dioxygen complex, and (d) PdO_3^+ with 2 CO molecules and attacking the dioxygen complex.

form of dioxygen is the superoxide (O_2^-) which is negatively charged, as CO is strongly electron withdrawing an O_2 unit is left containing limited electron density which presents lowered activity. The binding of the second CO is weaker than the first, so the CO ability to insert into the dioxygen site is reduced. The electron withdrawing nature of CO slightly deactivates the dioxygen complex, both by weakening the second CO bond and increasing the strength of the O–O bond. The effect is relatively small in the 1 μ_b case, but is quite pronounced in the cases with 3 μ_b. The addition of O in going from PdO_2^+ to PdO_3^+ results in a more complicated situation because the O radical site pulls both charge and spin from the dioxygen complex resulting in reaction barriers that are similar to PdO_2^+. The 3 μ_b reaction profiles in which CO attacks the dioxygen site are less reactive than lower spin states and CO slightly increases the barrier heights for dioxygen sites, especially for the high spin states.

The cooperative reactivity observed in the radical O sites has also been examined; we find different behaviors, which depend on the cooperative compound and spin. O radical sites with a larger spin multiplicity are generally found to be more reactive. The exception to this is the high energy isomer of $^2PdO_2^+$ which has a distorted structure, in which the O atoms are not equivalent, one has a large local spin moment of 1.12 μ_b, while the other has a short Pd–O bond and a moment of −0.75 μ_b. The result is that the $^2PdO_2^+$ with a broken O–O bond has a lower barrier for reacting with CO than the high energy isomer $^4PdO_2^+$ with the O–O bond broken, however, this is not a likely reaction pathway as the PdO_2^+ isomer containing radical oxygen is much higher in energy. In all other cases, the quartet potential energy surface has a lower barrier than the doublet potential energy surface when considering the radical site. The second trend is that the binding of an additional CO increases the barrier in all cases. We note that the binding of the additional CO increases the kinetic energy of system by far more than the barrier is increased, so we expect enhanced reactivity with the binding of two CO molecules in the gas-phase. The increase in the barrier height is most likely due to the reduced binding energy of the second CO molecule that increases the potential energy surface of the reaction. While the effect on the oxygen atom seems to be small, the binding of the second CO molecule is consistently weaker than the first, averaging 1.7 eV for the first CO and 1.0–1.3 eV for the second CO. As the barriers are related to both the radical site and the binding strength of the CO, this is likely to cause a higher barrier for reaction pathways which bind two CO molecules.

CONCLUSIONS

Through a combination of experiments in the gas-phase and theoretical investigations, we have evaluated the

reactivity of PdO_n^+ clusters in the oxidation of CO to understand how changing the type of oxygen center, spin, and functional groups attached to the Pd atom effect the reactivity. PdO_2^+ is found to have a ground state structure with a dioxygen complex, and PdO_3^+ is found to have both a radical oxygen center and an adsorbed dioxygen molecule. CO oxidation products with an additional CO bound to the product are observed in the experiments suggesting that cooperative reactivity is playing an important role in the oxidation of CO to CO_2. Theoretical investigations reveal that the cooperative reactivity is stimulated through putting additional kinetic energy into the reaction, as the binding of multiple CO molecules increases the barrier to reactivity in nearly all cases. The decrease in reactivity is due to the electron withdrawing nature of CO, which reduces the binding energy of the second CO molecule which shifts up the potential energy surface of the reaction as compared to the surface with only one CO molecule. This process is analogous with the effect seen in surfaces where oxygen binding to palladium surfaces decreases markedly as the surface is covered with electron withdrawing oxygen. We also investigated the role of spin and found that two-state reaction mechanisms may play a small role in the reactivity, but it is not as significant as in other studies of transition metal catalysis. This investigation of gas-phase reactivity allows a comprehensive study of cooperative effects in the oxidation of CO to CO_2 and shows how the addition of electron withdrawing groups, spin, and types of activated oxygen affect the reactivity giving suggestions on how the reactivity may be manipulated.

ACKNOWLEDGMENTS

This material is based upon work supported by the Air Force Office of Scientific Research (AFOSR) Award No FA9550-08-01-0400.

[1]H. Conrad, G. Ertl, and J. Küppers, J. Surf. Sci. **76**, 323 (1978).
[2]T. Engel and G. Ertl, J. Chem. Phys. **69**, 1267 (1978).
[3]S. Kunz, F. F. Schweinberger, V. Habibpour, M. Röttinger, C. Harding, M. Arenz, and U. Heiz, J. Phys. Chem. C **114**, 1651 (2010).
[4]D. Ciuparu, M. R. Lyubovsky, E. Altman, L. D. Pfefferle, and A. Datye, Catal. Rev. **44**, 593 (2002).
[5]P. O. Thevenin, E. Pocoroba, L. J. Pettersson, H. Karhu, I. J. Väyrynen, and S. G. Järkás, J. Catal. **207**, 139 (2002).
[6]T. Shimizu, A. D. Abid, G. Poskrebyshev, H. Wang, J. Nabity, J. Engel, J. Yu, D. Wickham, B. van Devener, S. L. Anderson, and S. Williams, Combust. Flame **157**, 421 (2010).
[7]T. Shimizu and H. Wang, Proc. Combust. Inst. **33**, 1859 (2011).
[8]W. Y. Huang, J. H. C. Liu, P. Alayoglu, Y. M. Li, C. A. Witham, C. K. Tsung, F. D. Toste, and G. A. Somorjai, J. Am. Chem. Soc. **132**, 16771 (2010).
[9]G. A. Somorjai and C. Aliaga, Langmuir **26**, 16190 (2010).
[10]G. A. Somorjai, Science **322**, 932 (2008).
[11]E. C. Tyo, A. W. Castleman, Jr., A. C. Reber, and S. N. Khanna, J. Phys. Chem. C **115**, 16797 (2011).
[12]J. U. Reveles, G. E. Johnson, S. N. Khanna, and A. W. Castleman, Jr., J. Phys. Chem. C **114**, 5438 (2009).
[13]N. M. Reilly, J. U. Reveles, G. E. Johnson, S. N. Khanna, and A. W. Castleman, Jr., J. Phys. Chem. A **111**, 4158 (2007).
[14]G. E. Johnson, R. Mitrić, M. Nössler, E. C. Tyo, V. Bonačić-Koutecký, and A. W. Castleman, Jr., J. Am. Chem. Soc. **131**, 5640 (2009).
[15]A. W. Castleman, Jr. and S. N. Khanna, J. Phys. Chem. C **113**, 2664 (2009).
[16]R. E. Leuchtner, A. C. Harms, and A. W. Castleman, Jr., J. Chem. Phys. **91**, 2753 (1989).
[17]D. E. Bergeron, P. J. Roach, A. W. Castleman, Jr., N. O. Jones, and S. N. Khanna, Science **307**, 231 (2005).
[18]P. J. Roach, W. H. Woodward, A. W. Castleman, Jr., A. C. Reber, and S. N. Khanna, Science **323**, 492 (2009).
[19]A. C. Reber, S. N. Khanna, P. J. Roach, W. H. Woodward, and A. W. Castleman, Jr., J. Phys. Chem. A **114**, 6071 (2010).
[20]A. C. Reber, S. N. Khanna, P. J. Roach, W. H. Woodward, and A. W. Castleman, Jr., J. Am. Chem. Soc. **129**, 16098 (2007).
[21]W. E. Kaden, T. P. Wu, W. A. Kunkel, and S. L. Anderson, Science **326**, 826 (2009).
[22]W. E. Kaden, W. Kunkel, M. Kane, F. Roberts, and S. L. Anderson, J. Am. Chem. Soc. **132**, 13097 (2009).
[23]S. V. Ong and S. N. Khanna, J. Phys. Chem. C **115**, 20217 (2011).
[24]G. E. Johnson, R. Mitrić, E. C. Tyo, V. Bonačić-Koutecký, and A. W. Castleman, Jr., J. Am. Chem. Soc. **130**, 13912 (2008).
[25]D. R. Justes, R. Mitrić, N. A. Moore, V. Bonačić-Koutecký, and A. W. Castleman, Jr., J. Am. Chem. Soc. **125**, 6289 (2003).
[26]E. C. Tyo, M. Nössler, R. Mitrić, V. Bonačić-Koutecký, and A. W. Castleman, Jr., Phys. Chem. Chem. Phys. **13**, 4243 (2011).
[27]S. Feyel, D. Schröder, and H. Schwartz, J. Phys. Chem. A **110**, 110 (2006).
[28]S. Feyel, D. Döbbler, R. Hokendorf, M. K. Beyer, J. Sauer, and H. Schwartz, Angew. Chem., Int. Ed. **47**, 1946 (2008).
[29]D. Schröder, S. Shaik, and H. Schwarz, Acc. Chem. Res. **33**, 139 (2000).
[30]B. Huber, H. Häkkinen, U. Landman, and M. Moseler, Comput. Mater. Sci. **35**, 371 (2006).
[31]B. Kalita and R. C. Deka, J. Am. Chem. Soc. **131**, 13252 (2009).
[32]F. Mehmood, J. Greeley, and L. A. Curtiss, J. Phys. Chem. C **113**, 21789 (2009).
[33]J. Hagen, L. D. Socaciu, J. Le Roux, D. Popolan, T. M. Bernhardt, L. Wöste, R. Mitrić, H. Noack, and V. Bonočić-Koutecký, J. Am. Chem. Soc. **126**, 3442 (2004).
[34]R. C. Bell, K. A. Zemski, D. R. Justes, and A. W. Castleman, Jr., J. Chem. Phys. **114**, 798 (2001).
[35]R. C. Bell and A. W. Castleman, Jr., J. Phys. Chem. A **106**, 9893 (2002).
[36]A. M. Köster, P. Calaminici, M. E. Casida, R. Flores-Moreno, G. Geudtner, A. Goursot, T. Heine, A. Ipatov, F. Janetzko, J. M. del Campo, S. Patchkovskii, J. U. Reveles, D. R. Salahub, and A. Vela, deMon2k. The deMon Developers, Cinvestav, Mexico (2010); see http://www.deMon-software.com.
[37]J. P. Perdew, K. Burke, and M. Enzerhof, Phys. Rev. Lett. **77**, 3865 (1996).
[38]J. M. L. Martin and A. Sunderman, J. Chem. Phys **114**, 3408 (2001).
[39]D. Andrae, U. Haeussermann, M. Dolg, H. Stoll, and H. Preuss, Theor. Chim. Acta **77**, 123 (1990).
[40]A. M. Köster, P. Calaminici, E. Orgaz, D. R. Roy, J. U. Reveles, and S. N. Khanna, J. Am. Chem. Soc. **133**, 12192 (2011).
[41]N. Godbout, D. R. Salahub, J. Andzelm, and E. Wimmer, Can. J. Chem. **70**, 560 (1992).
[42]J. M. del Campo and A. M. Köster, J. Chem. Phys. **129**, 024107 (2008).
[43]See supplementary material at http://dx.doi.org/10.1063/1.3669428 for graph of energy with respect to O–Pd–O bond angle for PdO_2^+ and $OCPdO_2^+$.
[44]S. L. Anderson, personal communication (2011).